On dynamics of origami-inspired rod

Abstract

We discuss the dynamics of a relatively simple origami-inspired structure considering discrete and continuum models. The latter was derived as a certain limit of the discrete model. Here we analyze small in-plane deformations and related equations of infinitesimal motions. For both models, dispersion relations were derived and compared. The comparison of the dispersion relations showed that the continuum model can capture the behavior of origami structures, which can be helpful in the materials properties determination and nondestructive evaluation.

Keywords: origami structure, dynamics, dispersion relations, continuum model, wave propagation

Introduction

The interest in a new class of composite materials called metamaterials is rapidly growing. It reflects their attractive properties, see, e.g., Cui et al. (2016); Lakes (2020); Choudhury (2022). Among various types of metamaterials, such ones as origami/kirigami structures are worth mentioning. In addition to their aesthetic properties, these materials found many applications in soft robotics, reconfigurable and self-folding structures, see, e.g., Silverberg et al. (2014); Mukhopadhyay et al. (2020); Yasuda et al. (2016, 2019); Novelino et al. (2020).

Here we discuss the in-plane dynamic behavior of a one-dimensional origami-inspired folding rod. Considering such structures, one may use various modeling approaches. The first one can be called discrete as it is similar to lattice dynamics, whereas the second is related to introducing a continuum model with effective properties. In the following, we use and compare both approaches. For modeling of microstructured media and their applications, we also refer to Cehula & Průša (2020); Adhikari et al. (2020); Chen et al. (2023); Mahoney & Siegmund (2022); Wang et al. (2021); Boni & Royer-Carfagni (2021).

The discrete representation of origami-inspired beam is essentially a one-dimensional mass-spring chain. Relative simplicity of such kind of models caused their extensive use to represent classical and non-classical elastic media. Dynamics of classical elastic media obtained from chain models and some generalizations (anticontinuum limit, splashes, higher-order approximation) were reviewed in Andrianov et al. (2010). One-dimensional models of solids with non-local interactions were considered in Kunin (2012); Andrianov & Awrejcewicz (2005), dynamics of discrete gradient elasticity models were studied in Metrikine & Askes (2002); Askes & Metrikine (2002), the media with microrotations can be found at Lisina et al. (2001); Ostoja-Starzewski (2002). It must be noted that one-dimensional models can be also successfully used in qualitative description of complicated physical processes such as crack propagation in brittle solids Slepyan & Troyankina (1984); Cherkaev et al. (2005); Berinskii & Slepyan (2017); Gorbushin & Mishuris (2017, 2019); Kazarinov et al. (2022), and thermoelasticity (see e.g Podolskaya et al. (2022) and the references therein).

We consider the origami structure as an elastic network consisting of axial and torsional springs, see Fig. 1. Such an approach was successfully used before to simulate lattice mechanical metamaterials (Berinskii, 2016) and periodic structures (Norris, 2014; Eremeyev, 2019; Eremeyev & Reccia, 2022). However, these works have not considered discrete dynamical equations of motion for the elements of the structures. At the same time, such equations were obtained for the elastic networks simulating atoms of crystal lattice (Berinskii & Kuzkin, 2020; Panchenko et al., 2022). Here, we use a similar way but apply it to the origami-like periodic structure. Obviously, a structure shown in Fig. 1 has some similarities with triangular and cubic lattices, see e.g. Carta et al. (2023); Nieves et al. (2020, 2013, 2022); Sharma (2022); Lal Sharma & Mishuris (2020); Eremeyev & Sharma (2019) and the reference therein. In fact, here we have a row of triangular or cubic lattice but with additional rotational springs. In the following we demonstrate that the latter play an essential role.

The paper is organized as follows. First, we consider a discrete origami-like structure. Considering equations of motion, we obtain dispersion relations. Then, we introduce a continuum limit of the discrete system and again derive dispersion relations. The comparison of the latter with the discrete models demonstrates that the continuum model has the same dynamic properties. Finally, in order to compare the continuum model with other enhanced models of continua, we re-write equations of motion introducing a

new set of dependent variables.

1. Analysis of discrete system

In the following we consider the origami rod consisting of equal links of initial length a, see Fig. 1. Each link is represented as two equal masses M concentrated on its ends. The nearest masses are connected with axial springs of stiffness c and angular springs of stiffness γa^2. For each elementary cell we have four degrees of freedom corresponding to the displacements of each mass along two directions: U_x, U_y, V_x, V_y.

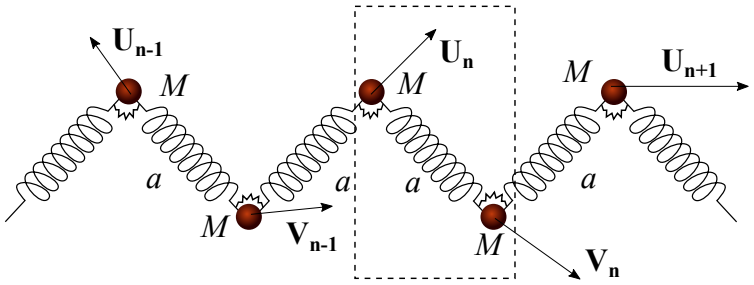

Figure 1: A part of a origami rod. nth elementary cell is framed

1.1. Equations of motion for discrete system

First, let us consider a discrete model within the framework of the Lagrange–Euler formalism, see e.g. Lurie (2001). So equations of motion of the unit cell have the form:

$$\frac{\mathrm{d}}{\mathrm{d}t}\frac{\partial K}{\partial \dot{q}_n^i} - \frac{\partial K}{\partial q_n^i} = -\frac{\partial W}{\partial q_n^i}, \qquad \mathbf{q}_n = \begin{bmatrix} U_n^x & U_n^y & V_n^x & V_n^y \end{bmatrix}^{\mathrm{T}}, \tag{1}$$

where U_n^x, U_n^y, V_n^x, V_n^y are components of displacement vectors $\mathbf{U}_n$, $\mathbf{V}_n$ in Cartesian basis; q_n^i, $i = 1, 2, 3, 4$, is the i-th component of column $\mathbf{q}_n$; K is the total kinetic energy of the unit cell; W is an elastic energy related to lattice particles motion $\mathbf{U}_n$, $\mathbf{V}_n$. Hereinafter vectors and matrices are denoted by bold symbols.

The total kinetic energy of the unit cell is calculated as

$$K = \frac{1}{2}M(\dot{\mathbf{U}}_n^2 + \dot{\mathbf{V}}_n^2). \tag{2}$$

Potential energy W is equal to a sum of energies of all linear and angular springs connected with particles of nth unit cell:

$$W = W^{ax} + W^{tor}. \tag{3}$$

Here W^{ax} and W^{tor} stand for contributions of axial and torsional springs respectively. The expression for W^{ax} in harmonic approximation has form

$$\begin{aligned} W^{ax} = \frac{c}{2a^2}\Big[\big(\mathbf{a}_1 \cdot (\mathbf{U}_n - \mathbf{V}_n)\big)^2 + \big(\mathbf{a}_2 \cdot (\mathbf{U}_n - \mathbf{V}_{n-1})\big)^2 \\ + \big(\mathbf{a}_2 \cdot (\mathbf{U}_{n+1} - \mathbf{V}_n)\big)^2\Big]. \end{aligned} \tag{4}$$

Here dot stands for the scalar product, and $\mathbf{a}_1$ and $\mathbf{a}_2$ are vectors of length a directed along springs.

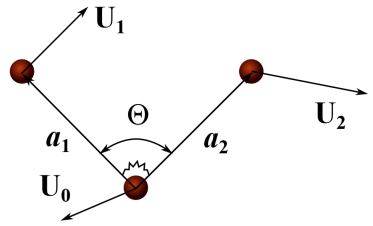

Figure 2: A torsional spring between two arbitrary links

Angular part of the potential energy, W^{tor} per n-th elementary cell, is determined by change of 4 angles depending on displacements $\mathbf{U}_n$ and $\mathbf{V}_n$. The following expression for W^{tor} is used

$$W^{tors} = \sum_{i=1}^{4} \Pi_i^{tor}, \qquad \Pi_i^{tor} = \frac{1}{2}\gamma a^2(\Theta_i - \Theta_i^0)^2. \tag{5}$$

Let us consider the specific torsional spring. Assume that the spring connects two links at the joint such that the initial angle between the links is equal to Θ_i^0 (Fig. 2). The other ends of the links are initially set by relative position vectors $\mathbf{a}_1$ and $\mathbf{a}_2$ such that $|\mathbf{a}_1| = |\mathbf{a}_2| = a$. Assume that the joint have the displacement $\mathbf{U_0}$ while the ends of the links have displacements $\mathbf{U_1}$ and $\mathbf{U_2}$ respectively. As a result, the angle between the links is changed to Θ_i such that the Tailor expansion gives:

$$\cos(\Theta_i - \Theta_i^0) \approx 1 - \frac{1}{2}(\Theta_i - \Theta_i^0)^2 \tag{6}$$

Corresponding change of the potential energy is

$$\Pi_i^{tor} \approx \gamma(1 - \cos\Theta_i \cos\Theta_i^0 - \sin\Theta_i \sin\Theta_i^0) \tag{7}$$

Consideration of the displacements of the links gives the relation for the cosine:

$$\cos\Theta = \frac{(\mathbf{a}_1 + \mathbf{U}_1 - \mathbf{U}_0) \cdot (\mathbf{a}_2 + \mathbf{U}_2 - \mathbf{U}_0)}{|\mathbf{a}_1 + \mathbf{U}_1 - \mathbf{U}_0||\mathbf{a}_2 + \mathbf{U}_2 - \mathbf{U}_0)|}, \tag{8}$$

while $\sin\Theta = \sqrt{1 - \cos^2\Theta}$. The energies of all considered angular springs are calculated similarly. The obtained relations for $\cos\Theta$ and $\sin\Theta$ are represented with Taylor expansion such that the terms up to the second order are kept in the relations of the total potential and kinetic energy in the unit cell.

Hereinafter we restrict ourselves to value $\Theta_0 = \pi/2$. Substituting expressions for kinetic and potential energies into Lagrange-Euler equation (1), we get equations of motion for the unit cell:

$$\begin{aligned}
M\ddot{U}_x^n &= \tfrac{1}{2}\Big(c\,(2U_x^n - V_x^{n-1} - V_y^{n-1} - V_x^n + V_y^n) \\
&\quad -\gamma\,(U_x^{n-1} + U_y^{n-1} + U_x^{n+1} - U_y^{n+1} - 2U_x^n - 2V_y^{n-1} + 2V_y^n)\Big), \\
M\ddot{U}_y^n &= \tfrac{1}{2}\Big(c\,(2U_y^n - V_x^{n-1} - V_y^{n-1} + V_x^n - V_y^n) \\
&\quad -\gamma(U_x^{n-1} + U_y^{n-1} - U_x^{n+1} + U_y^{n+1} + 6U_y^n + 2V_x^{n-1} \\
&\quad -4V_y^{n-1} - 2V_x^n - 4V_y^n)\Big), \\
M\ddot{V}_x^n &= \tfrac{1}{2}\Big(-c\,(U_x^{n+1} + U_y^{n+1} + U_x^n - U_y^n - 2V_x^n) \\
&\quad +\gamma\,(2U_y^{n+1} - 2U_y^n - V_x^{n-1} + V_y^{n-1} - V_x^{n+1} - V_y^{n+1} + 2V_x^n)\Big), \\
M\ddot{V}_y^n &= \tfrac{1}{2}\Big(-c\,(U_x^{n+1} + U_y^{n+1} - U_x^n + U_y^n - 2V_y^n) \\
&\quad +\gamma\,(2U_x^{n+1} - 4U_y^{n+1} - 2U_x^n - 4U_y^n - V_x^{n-1} \\
&\quad +V_y^{n-1} + V_x^{n+1} + V_y^{n+1} + 6V_y^n)\Big).
\end{aligned} \tag{9}$$

1.2. Dispersion relations

Let us derive dispersion relation for the discrete origami beam corresponding to (9). We seek for solution of (9) in a form of propagating one-dimensional wave:

$$\mathbf{U}_n = \mathbf{U}e^{i(kln - \omega t)}, \qquad \mathbf{V}_n = \mathbf{V}e^{i(kln - \omega t)}, \tag{10}$$

where $\mathbf{U}, \mathbf{V}$ are the amplitudes of the waves; ω is a frequency; k is a wavenumber;

$$l = 2\sin\left(\frac{\Theta_0}{2}\right) a = \sqrt{2}a \tag{11}$$

is a unit cell length.

Using a formula (10), we represent equations of motion (9) in the matrix form

$$\mathbf{M}\ddot{\mathbf{q}}_n + \mathbf{C}\mathbf{q}_n = 0, \qquad \mathbf{M} = M\mathbf{E}, \tag{12}$$

where $\mathbf{C}$ and $\mathbf{M}$ are 4×4 stiffness and mass matrices, respectively; $\mathbf{E}$ is 4×4 identity matrix; vector $\mathbf{q}_n$ is a vector of displacements defined in (1).

Taking (10) into account, we obtain from (12) homogeneous system of linear equations with respect to $\mathbf{q}_{n,m}$:

$$\left(\mathbf{C}(k) - \omega^2\mathbf{M}\right)\mathbf{q}_{n,m} = 0. \tag{13}$$

The system has non-trivial solutions under the following condition:

$$\det\left(\mathbf{\Omega}(k) - \omega^2\mathbf{E}\right) = 0, \qquad \mathbf{\Omega}(k) = \frac{1}{M}\mathbf{C}, \tag{14}$$

where $\mathbf{\Omega}$ can be referred to as the dynamical matrix (Dove (1993)). Solution of the fourth order equation (14) with respect to ω^2 yields dispersion relations $\omega = \omega_i(k), i = 1, 2, 3, 4$, shown in Figs. 3 and 4. Here we used the following dimensionless values: $M = 1$, $a = 1$. Taking account the symmetry of the chain, we plot the dispersion relations on the interval $-\frac{\pi}{l} < k < \frac{\pi}{l}$ corresponding to the first Brillouin zone of the considered system.

2. Waves in the equivalent continuum

2.1. Continuum limit

Let us consider equations of motion (9) corresponding to the system representing the origami rod. Let us approximate the discrete functions (10) as

$$\begin{aligned} U_x^{n\pm1} &\approx u_x \pm u_x' l + \tfrac{1}{2}u_x'' l^2, \qquad & V_x^{n\pm1} &\approx v_x \pm v_x' l + \tfrac{1}{2}v_x'' l^2, \\ U_y^{n\pm1} &\approx u_y \pm u_y' l + \tfrac{1}{2}u_y'' l^2, \qquad & V_y^{n\pm1} &\approx v_y \pm v_y' l + \tfrac{1}{2}v_y'' l^2, \end{aligned} \tag{15}$$

where the $u_x(x,t), u_y(x,t), v_x(x,t), v_y(x,t)$ are assumed to be the smooth enough continuous functions, $()' = \frac{\partial}{\partial x}$.

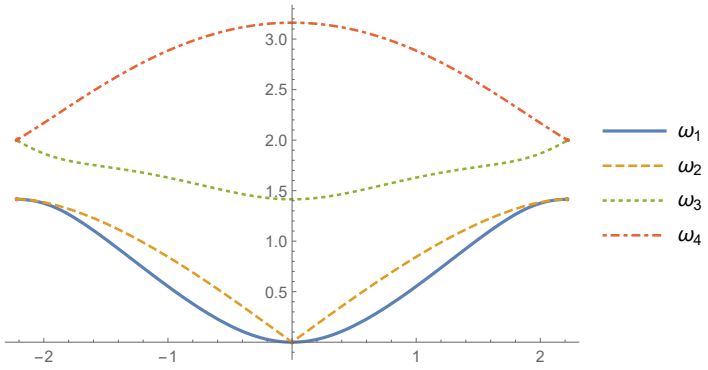

Figure 3: Dispersion relations $\omega(k)$. $\frac{c}{\gamma} = 1$

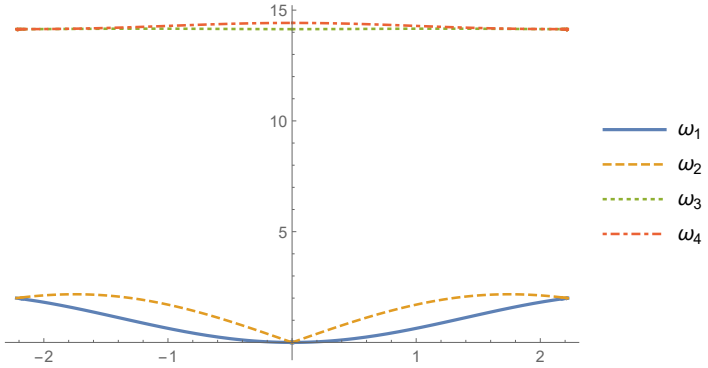

Figure 4: Dispersion relations $\omega(k)$. $\frac{c}{\gamma} = 100$

Substitution (15) into (9) allows us to obtain the following system of

partial differential equations:

$$\begin{gathered}
M\ddot{u}_x + c(u_x - v_x) - \tfrac{1}{2}a^2\Big(c(v''_x + v''_y) + 2\gamma(u''_x - v''_y)\Big) \\
+\sqrt{2}a\Big(c(v'_x + v'_y) + 2\gamma(u'_y - v'_y)\Big) = 0, \\
M\ddot{u}_y + (u_y - v_y)(c + 4\gamma) - \tfrac{1}{2}a^2\Big(c(v''_x + v''_y) - 2(u''_y + v''_x - 2v''_y)\gamma\Big) \\
+\sqrt{2}a\Big(c(v'_x + v'_y) - 2\gamma(u'_x + v'_x - 2v'_y)\Big) = 0, \\
M\ddot{v}_x - c(u_x - v_x) - \tfrac{1}{2}a^2\Big(c(u''_x + u''_y) - 2\gamma(u''_y - v''_x)\Big) \\
-\sqrt{2}a\Big(c(u'_x + u'_y) - 2\gamma(u'_y - v'_y)\Big) = 0, \\
M\ddot{v}_y - (u_y - v_y)(c + 4\gamma) - \tfrac{1}{2}a^2(c(u''_x + u''_y) - 2\gamma(u''_x - 2u''_y + v''_y)) \\
-\sqrt{2}a\Big(c(u'_x + u'_y) - 2\gamma(u'_x - 2u'_y + v'_x)\Big) = 0.
\end{gathered} \tag{16}$$

We are looking for the solutions of this system of equations in the form

$$u_{x,y} = U_{x,y}e^{i(\omega t - klx)}, \qquad v_{x,y} = V_{x,y}e^{i(\omega t - klx)}. \tag{17}$$

As a result, we get a following matrix equation

$$\mathbf{KY} = \mathbf{0}, \qquad \mathbf{Y} = \begin{pmatrix} U_x & U_y & V_x & V_y \end{pmatrix}^{\mathrm{T}}. \tag{18}$$

Here

$$\mathbf{K} = \begin{pmatrix}
a^2\gamma k^2 + c - M\omega^2 & i\sqrt{2}a\gamma k & \frac{1}{2}c\left(a^2k^2 + i\sqrt{2}ak - 2\right) & \frac{1}{2}ak\left(ak + i\sqrt{2}\right)(c - 2\gamma) \\
-i\sqrt{2}a\gamma k & \gamma\left(4 - a^2k^2\right) + c - M\omega^2 & \frac{1}{2}ak\left(ak + i\sqrt{2}\right)(c - 2\gamma) & \frac{1}{2}\left(a^2k^2 + i\sqrt{2}ak - 2\right)(c + 4\gamma) \\
\frac{1}{2}c\left(a^2k^2 - i\sqrt{2}ak - 2\right) & \frac{1}{2}ak\left(ak - i\sqrt{2}\right)(c - 2\gamma) & a^2\gamma k^2 + c - M\omega^2 & -i\sqrt{2}a\gamma k \\
\frac{1}{2}ak\left(ak - i\sqrt{2}\right)(c - 2\gamma) & \frac{1}{2}\left(a^2k^2 - i\sqrt{2}ak - 2\right)(c + 4\gamma) & i\sqrt{2}a\gamma k & \gamma\left(4 - a^2k^2\right) + c - M\omega^2
\end{pmatrix}. \tag{19}$$

is a Hermitian matrix, meaning that its eigenvalues are real at any combination of c and γ. System of linear equations (18) has non-trivial solutions if $\det \mathbf{K} = 0$. The last conditions give the dispersion relations for the equivalent continuum. The latter are shown in Fig. 5 – 7, where the comparison with those obtained for the discrete system.

2.2. Equivalent Equations of motion

Let us analyze the system of equations (16). We introduce new variables

$$r_x = \frac{u_x + v_x}{2} \qquad r_y = \frac{u_y + v_y}{2}. \tag{20}$$

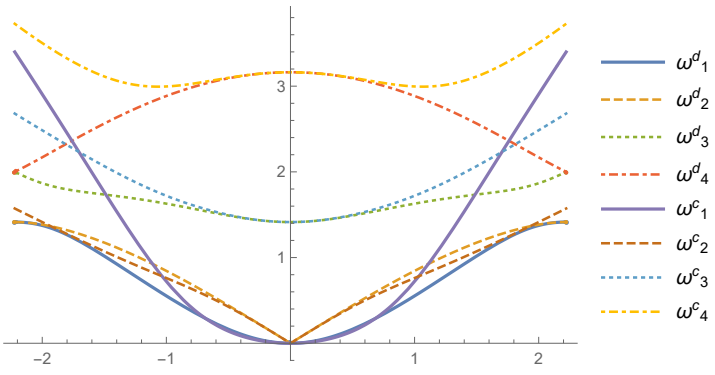

Figure 5: Dispersion relations $\omega(k)$. $\frac{c}{\gamma} = 1$

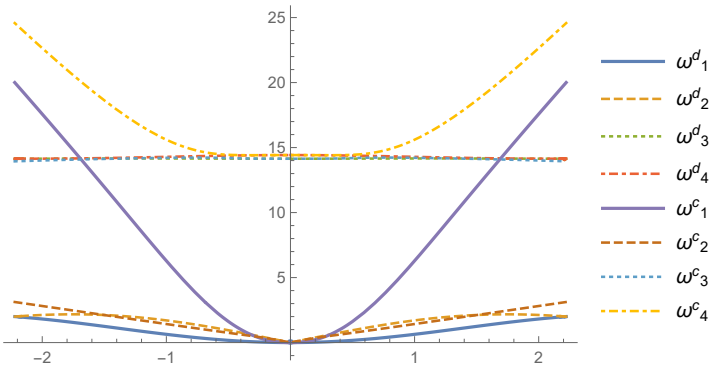

Figure 6: Dispersion relations $\omega(k)$. $\frac{c}{\gamma} = 100$

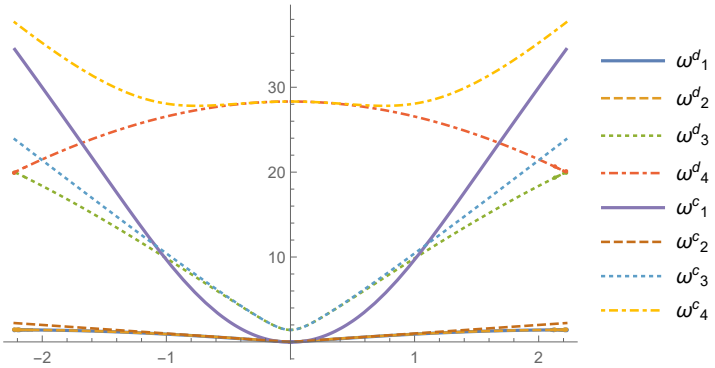

Figure 7: Dispersion relations $\omega(k)$. $\frac{c}{\gamma} = 0.01$

These are continuum functions associated with the motion of the center of mass of the specific link of the discrete system. Another variable

$$\varepsilon = \frac{1}{a}(\mathbf{u} - \mathbf{v}) \cdot \frac{\mathbf{a}_1}{a} = \frac{1}{\sqrt{2}a}\Big((V_x - U_x) - (V_y - U_y)\Big) \tag{21}$$

stands for the microscopic strain of the link. Finally, let us introduce the variable corresponding to the single link rotation. Using the formula

$$\sin\varphi = \frac{\mathbf{a}_1 \times (\mathbf{u} - \mathbf{v} + \mathbf{a}_1)}{|\mathbf{a}_1||\mathbf{u} - \mathbf{v} + \mathbf{a}_1|}, \tag{22}$$

we obtain

$$\varphi \approx \frac{\mathbf{a}_1 \times (\mathbf{u} - \mathbf{v} + \mathbf{a}_1)}{a^2} = \frac{1}{\sqrt{2}a}\Big((V_x - U_x) + (V_y - U_y)\Big). \tag{23}$$

Combining (16) we get an equivalent system with respect to new variables:

$$\begin{aligned}
&2M\ddot{r_x} - a^2\big(c(r_x'' + r_y'' - \varphi') + 2\gamma(r_x'' - r_y'' + \varphi' - \varepsilon')\big) = 0,\\
&2M\ddot{r_y} - a^2\left(c(r_x'' + r_y'' - \varphi') - 2\gamma(r_x'' - r_y'' + \varphi' - \varepsilon')\right) = 0,\\
&M\ddot{\varphi} - 2\ c\ (r_x' + r_y' - \varphi) + 4\gamma(r_x' - r_y' + \varphi - \varepsilon)\\
&\qquad +a^2(c\varphi'' - 2\gamma\varepsilon'') = 0,\\
&M\ddot{\varepsilon} + 2c\varepsilon + 2a^2\gamma(\varepsilon'' - \varphi'') - 4\gamma(r_x' - r_y' + \varphi - \varepsilon) = 0.
\end{aligned} \tag{24}$$

Let us now introduce for the considered structure A as a section area, $\rho A = \sqrt{2}M/a$ as specific mass, $\rho I = \sqrt{2}Ma$ as a section moment of inertia. We also introduce an axial stiffness by relation $c = \sqrt{2}C_1A/a$, and the bending stiffness using $\gamma = \sqrt{2}C_2A/(2a)$.

Then equivalent continuum describing the motion of the origami rod is represented by the system of equations:

$$\begin{aligned}
&\rho A\ddot{r_x} - C_1A(r_x'' + r_y'' - \varphi') - C_2A(r_x'' - r_y'' + \varphi' - \varepsilon') = 0,\\
&\rho A\ddot{r_y} - C_1A(r_x'' + r_y'' - \varphi') + C_2A(r_x'' - r_y'' + \varphi' - \varepsilon') = 0,\\
&\rho I\ddot{\varphi} - 4\ AC_1\ (r_x' + r_y' - \varphi) + 4AC_2(r_x' - r_y' + \varphi - \varepsilon)\\
&\qquad +2Aa^2(C_1\varphi'' - C_2\varepsilon'') = 0,\\
&\rho Aa^2\ddot{\varepsilon} + 4AC_1\varepsilon + 2Aa^2C_2(\varepsilon'' - \varphi'') - 4AC_2(r_x' - r_y' + \varphi - \varepsilon) = 0.
\end{aligned} \tag{25}$$

Results and conclusions

Discrete dispersion relations on Fig. 3 and Fig. 4 reveal two acoustic and two optical curves. The bandgap zones between the waves of different

types arises with an increase of the relation between the axial and torsional stiffness. Let us note that the bandgap phenomenon may be observed in different types of one-dimensional chains. For example, Kunin (2012) shows that the equations of the diatomic chain coincide with those of Cosserat-type chain. Both of them have optical curves in addition to the acoustic ones, and hence on some frequencies waves' propagation is not possible. Introduction of the torsional springs in our model takes rotational degrees of freedom into account similarly to as it is done in Cosserat model. However, as we take the axial stiffness into account, our model becomes more general and has four degrees of freedom unlike Cosserat model with the two ones. One can expect that in case of rigid links our model would be qualitatively identical to the Cosserat model but this question is out of the scope of the current work.

Figures 5–7 show relation between the discrete and continuous dispersion curves. One can observe the limits of the long-wave approximation for accurate description of the dynamics of the system with the corresponding continuum model. Qualitatively, the trends of the discrete and continual curves are similar for $0 < ka < \frac{1}{2}$ in all three considered cases. However it must be noted that the optical waves are in general predicted better than the acoustic ones. For example in case of $ka = 0.5, \frac{c}{\gamma} = 0.01$, the value of the lowest continuum frequency is five times higher than this in discrete case, while the relative error for the highest optical frequencies at the same parameters does not exceeds 3%. Finally, we can conclude that the discrete model gives a richer picture of dispersion curves whereas a continuum approach coincides with discrete one in a certain range. In order to extend it one needs to consider approximations of higher order than (15).

In (25), we face four degrees of freedom related to in-plane displacements, rotation, and microstrain. Considering one-dimensional models of continua, the obtained system of equations is more general than Timoshenko or Cosserat kinematics and similar to the microstretch continuum model or one-dimensional micromorphic model by Eringen (1999), or any enhanced model with an additional scalar degree of freedom in a sense by Capriz (1989).

We presented both discrete and continuum models of an origami rod. Analyzing their acoustic properties, i.e., dispersion relations, we demonstrated an excellent coincidence in wave propagation of small amplitude within both models. Since the derived continuum model is relatively simpler, it could be more beneficial for practical applications. In particular, the continuum model may serve as a base for the non-destructive evaluation of flexible origami/kirigami structures. The same technique can be extended to an-

alyze prestressed structures within the incremental statement. One can see some similarities by comparing our continuum model with other models, such as Eringen's ones (Eringen, 1999). However, there is also a difference between our continuum, microstretch, and micromorphic ones. In another conclusion, microstructured media can be treated as a source of various enhanced models of continua or media with internal degrees of freedom. In fact, a microstructure may bring additional degrees of freedom (kinematical descriptors) and related governing equations.

Let us note that the presence of torsional springs plays an important role here. Indeed, they changed essentially the behaviour of dispersion curves in comparison with other studies, where only linear springs were considered. In other words, rotational interactions may be essential for discrete systems. Up to a certain order, this conclusion is similar to an influence of spinners in elastic systems (Carta et al., 2019; Nieves et al., 2020; Kandiah et al., 2023). As a result, the discussed model can be also used for modelling microsized structures such as polymeric chains and brushes, see e.g. Rigoberto & William J. Brittain (2004); Azzaroni & Szleifer (2018), but with links of variable length. Indeed, in this case we have interactions similar to dipole–dipole interactions such as described with the Stockmayer potential (Stockmayer, 1941) but with variable length of dipoles. So the considered model can be also considered as a certain extension of an approach based on the Stockmayer potential towards deformable diples of finite size.

References

Adhikari, S., Mukhopadhyay, T., Shaw, A., & Lavery, N. (2020). Apparent negative values of Young's moduli of lattice materials under dynamic conditions. *International Journal of Engineering Science*, *150*, 103231.

Andrianov, I. V., & Awrejcewicz, J. (2005). Continuous models for chain of inertially linked masses. *European Journal of Mechanics-A/Solids*, *24*, 532–536.

Andrianov, I. V., Awrejcewicz, J., Weichert, D. et al. (2010). Improved continuous models for discrete media. *Mathematical Problems in Engineering*, *2010*.

Askes, H., & Metrikine, A. V. (2002). One-dimensional dynamically consistent gradient elasticity models derived from a discrete microstructure: Part

2: Static and dynamic response. *European Journal of Mechanics-A/Solids*, *21*, 573–588.

Azzaroni, O., & Szleifer, I. (Eds.) (2018). *Polymer and Biopolymer Brushes: for Materials Science and Biotechnology*. Hoboken: Wiley.

Berinskii, I. (2016). Elastic networks to model auxetic properties of cellular materials. *International Journal of Mechanical Sciences*, *115*, 481–488.

Berinskii, I., & Kuzkin, V. (2020). Equilibration of energies in a two-dimensional harmonic graphene lattice. *Philosophical Transactions of the Royal Society A*, *378*, 20190114.

Berinskii, I. E., & Slepyan, L. I. (2017). How a dissimilar-chain system is splitting: quasi-static, subsonic and supersonic regimes. *Journal of the Mechanics and Physics of Solids*, *107*, 509–524.

Boni, C., & Royer-Carfagni, G. (2021). A nonlocal elastica inspired by flexural tensegrity. *International Journal of Engineering Science*, *158*, 103421.

Capriz, G. (1989). *Continua with Microstructure*. New York: Springer.

Carta, G., Nieves, M. J., & Brun, M. (2023). Lamb waves in discrete homogeneous and heterogeneous systems: Dispersion properties, asymptotics and non-symmetric wave propagation. *European Journal of Mechanics-A/Solids*, *100*, 104695.

Carta, G., Nieves, M. J., Jones, I. S., Movchan, N. V., & Movchan, A. B. (2019). Flexural vibration systems with gyroscopic spinners. *Philosophical Transactions of the Royal Society A*, *377*, 20190154.

Cehula, J., & Průša, V. (2020). Computer modelling of origami-like structures made of light activated shape memory polymers. *International Journal of Engineering Science*, *150*, 103235.

Chen, W., Wang, L., & Yan, Z. (2023). On the dynamics of curved magnetoactive soft beams. *International Journal of Engineering Science*, *183*, 103792.

Cherkaev, A., Cherkaev, E., & Slepyan, L. (2005). Transition waves in bistable structures. i. delocalization of damage. *Journal of the Mechanics and Physics of Solids*, *53*, 383–405.

Choudhury, P. K. (Ed.) (2022). *Metamaterials: Technology and Applications*. Boca Raton: CRC Press.

Cui, T. J., Tang, W. X., Yang, X. M., Mei, Z. L., & Jiang, W. X. (2016). *Metamaterials: Beyond Crystals, Noncrystals, and Quasicrystals*. Boca Raton: CRC Press.

Dove, M. T. (1993). *Introduction to lattice dynamics*. 4. Cambridge university press.

Eremeyev, V. A. (2019). Two-and three-dimensional elastic networks with rigid junctions: modeling within the theory of micropolar shells and solids. *Acta Mechanica*, *230*, 3875–3887.

Eremeyev, V. A., & Reccia, E. (2022). On dynamics of elastic networks with rigid junctions within nonlinear micro-polar elasticity. *International Journal for Multiscale Computational Engineering*, *20*, 1–11.

Eremeyev, V. A., & Sharma, B. L. (2019). Anti-plane surface waves in media with surface structure: Discrete vs. continuum model. *International Journal of Engineering Science*, *143*, 33–38.

Eringen, A. C. (1999). *Microcontinuum Field Theory. I. Foundations and Solids*. New York: Springer.

Gorbushin, N., & Mishuris, G. (2017). Analysis of dynamic failure of the discrete chain structure with non-local interactions. *Mathematical Methods in the Applied Sciences*, *40*, 3355–3365.

Gorbushin, N., & Mishuris, G. (2019). Dynamic fracture of a dissimilar chain. *Philosophical Transactions of the Royal Society A*, *377*, 20190103.

Kandiah, A., Jones, I. S., Movchan, N. V., & Movchan, A. B. (2023). Effect of gravity on the dispersion and wave localisation in gyroscopic elastic systems. In H. Altenbach, G. Bruno, V. A. Eremeyev, M. Y. Gutkin, & W. H. Müller (Eds.), *Mechanics of Heterogeneous Materials* (pp. 219–274). Cham: Springer International Publishing.

Kazarinov, N. A., Petrov, Y. V., & Gruzdkov, A. A. (2022). On dynamic fracture of one-dimensional elastic chain. In *Mechanics and Control of Solids and Structures* (pp. 303–314). Springer.

Kunin, I. A. (2012). *Elastic media with microstructure I: one-dimensional models* volume 26. Springer Science & Business Media.

Lakes, R. (Ed.) (2020). *Composites and Metamaterials*. Singapore: World Scientific.

Lal Sharma, B., & Mishuris, G. (2020). Scattering on a square lattice from a crack with a damage zone. *Proceedings of the Royal Society A*, *476*, 20190686.

Lisina, S., Potapov, A., & Nesterenko, V. (2001). A nonlinear granular medium with particle rotation: a one-dimensional model. *Acoustical Physics*, *47*, 598–606.

Lurie, A. I. (2001). *Analytical Mechanics*. Berlin: Springer.

Mahoney, K., & Siegmund, T. (2022). Mechanics of tubes composed of interlocking building blocks. *International Journal of Engineering Science*, *174*, 103654.

Metrikine, A. V., & Askes, H. (2002). One-dimensional dynamically consistent gradient elasticity models derived from a discrete microstructure: Part 1: Generic formulation. *European Journal of Mechanics-A/Solids*, *21*, 555–572.

Mukhopadhyay, T., Ma, J., Feng, H., Hou, D., Gattas, J. M., Chen, Y., & You, Z. (2020). Programmable stiffness and shape modulation in origami materials: Emergence of a distant actuation feature. *Applied Materials Today*, *19*, 100537.

Nieves, M. J., , A. B., Jones, I. S., & Mishuris, G. S. (2013). Propagation of Slepyan's crack in a non-uniform elastic lattice. *Journal of the Mechanics and Physics of Solids*, *61*, 1464–1488.

Nieves, M. J., Carta, G., Pagneux, V., & Brun, M. (2020). Rayleigh waves in micro-structured elastic systems: non-reciprocity and energy symmetry breaking. *International Journal of Engineering Science*, *156*, 103365.

Nieves, M. J., Livasov, P., & Mishuris, G. (2022). Dynamic fracture regimes for initially prestressed elastic chains. *Philosophical Transactions of the Royal Society A*, *380*, 20210395.

Norris, A. N. (2014). Mechanics of elastic networks. *Proceedings of the Royal Society A: Mathematical, Physical and Engineering Sciences*, *470*, 20140522.

Novelino, L. S., Ze, Q., Wu, S., Paulino, G. H., & Zhao, R. (2020). Untethered control of functional origami microrobots with distributed actuation. *Proceedings of the National Academy of Sciences*, *117*, 24096–24101.

Ostoja-Starzewski, M. (2002). Lattice models in micromechanics. *Appl. Mech. Rev.*, *55*, 35–60.

Panchenko, A. Y., Kuzkin, V., & Berinskii, I. (2022). Unsteady ballistic heat transport in two-dimensional harmonic graphene lattice. *Journal of Physics: Condensed Matter*, *34*, 165402.

Podolskaya, E. A., Krivtsov, A. M., & Kuzkin, V. A. (2022). Discrete thermomechanics: From thermal echo to ballistic resonance (a review). *Mechanics and Control of Solids and Structures*, (pp. 501–533).

Rigoberto, C. A., & William J. Brittain, J. R., Kenneth C. Caster (Eds.) (2004). *Polymer Brushes: Synthesis, Characterization, Applications*. Weinheim: Wiley.

Sharma, B. L. (2022). Surface wave across crack-tip in a lattice model. *Philosophical Transactions of the Royal Society A*, *380*, 20210396.

Silverberg, J. L., Evans, A. A., McLeod, L., Hayward, R. C., Hull, T., Santangelo, C. D., & Cohen, I. (2014). Using origami design principles to fold reprogrammable mechanical metamaterials. *science*, *345*, 647–650.

Slepyan, L., & Troyankina, L. (1984). Fracture wave in a chain structure. *Journal of Applied Mechanics and Technical Physics*, *25*, 921–927.

Stockmayer, W. H. (1941). Second virial coefficients of polar gases. *The Journal of Chemical Physics*, *9*, 398–402.

Wang, T., Liu, F., Fu, C., Zhang, X., Wang, K., & Xu, F. (2021). Curvature tunes wrinkling in shells. *International Journal of Engineering Science*, *164*, 103490.

Yasuda, H., Chong, C., Charalampidis, E. G., Kevrekidis, P. G., & Yang, J. (2016). Formation of rarefaction waves in origami-based metamaterials. *Physical Review E*, *93*, 043004.

Yasuda, H., Miyazawa, Y., Charalampidis, E. G., Chong, C., Kevrekidis, P. G., & Yang, J. (2019). Origami-based impact mitigation via rarefaction solitary wave creation. *Science advances*, *5*, eaau2835.